Journal of Magnetic Resonance **139,** 342–353 (1999)
Article ID jmre.1999.1778, available online at http://www.idealibrary.com on IDEAL®

Theory of Spin Echo in Restricted Geometries under a Step-wise Gradient Pulse Sequence

A. V. Barzykin[1]

National Institute of Materials and Chemical Research, Tsukuba, Ibaraki 305-8565, Japan

Received December 18, 1998; revised April 7, 1999

A closed matrix form solution of the Bloch–Torrey equation is presented for the magnetization density of spins diffusing in a bounded region under a steady gradient field and for the Stejskal–Tanner gradient pulse sequence, assuming straightforward generalization to any step-wise gradient profile. The solution is expressed in terms of the eigenmodes of the diffusion propagator in a given geometry with appropriate boundary conditions (perfectly reflecting or relaxing walls). Applications to rectangular, cylindrical, and spherical geometries are discussed. The relationship with the multiple propagator approach is established and an alternative step-wise gradient discretization procedure is suggested to handle arbitrary gradient waveforms.

Key Words: **pulsed-gradient spin-echo NMR; Bloch–Torrey equation; restricted diffusion.**

INTRODUCTION

Pulsed-gradient spin-echo NMR is a powerful method for studying molecular diffusion (*1–4*). In restricted geometries, the observable echo attenuation contains structural information about the confinement of the diffusing particles. By extracting this information from a suitably designed experiment one has been able to characterize various sophisticated morphologies, such as colloids (*5–7*), porous materials (*8–17*), and biological tissues (*18–21*).

Spin-echo phenomenology is well understood (*1–4*). Theoretically, the problem reduces to the solution of the so-called Bloch–Torrey equation (*22*) for the transverse magnetization density $m(\mathbf{r}, t)$ in a linear gradient field with appropriate boundary and initial conditions,

$$\frac{\partial}{\partial t} m(\mathbf{r}, t) = -igf(t)xm(\mathbf{r}, t) + D\nabla^2 m(\mathbf{r}, t), \qquad [1]$$

where D is the diffusion coefficient, g is the product of the gyromagnetic ratio and the gradient strength, $f(t)$ is the effective temporal shape function of the gradient, which is taken to be in the x direction. Exponential relaxation is factored out. The generalized gradient waveform $f(t)$ includes the effect of phase-inverting RF pulses which can be mimicked by switching over the sign of the gradient. The signal is proportional to the total magnetization,

$$M(t) = \int d\mathbf{r} m(\mathbf{r}, t). \qquad [2]$$

Equation [1] is derived in a usual way from the quantum evolution equation through the introduction of a stochastic term and conversion to the interaction representation.

Linearity of the gradient makes it possible to solve Eq. [1] in the continuum. For isotropic unrestricted diffusion (*23, 24*),

$$M(t) = \exp\left[-Dg^2 \int_0^t dt' \left(\int_0^{t'} dt'' f(t'') \right)^2 \right], \qquad [3]$$

where we have used the condition of complete spin rephasing, $\int_0^t dt' f(t') = 0$, realized in a typical experiment. We have also assumed that the signal is normalized, i.e., $M(0) = 1$. In the majority of the gradient NMR applications, one deals either with a steady gradient, $f_{SG}(t) = 1$, or with a two-pulse Stejskal–Tanner gradient profile (*23*),

$$f_{ST}(t) = -\theta(t) + \theta(t - \delta) + \theta(t - \Delta) - \theta(t - \Delta - \delta), \qquad [4]$$

where $\theta(t)$ is the Heaviside step function. Other pulse sequences are also used to satisfy particular purposes but the above two are the most common and, importantly, they capture all the essential features of the gradient NMR experiment. For the normalized signal in these cases, we have

$$M_{SG}(t) = \exp(-Dg^2t^3/3), \qquad [5]$$

$$M_{ST}(\Delta, \delta) = \exp[-Dg^2\delta^2(\Delta - \delta/3)]. \qquad [6]$$

No exact solution of Eq. [1] with an arbitrary gradient waveform $f(t)$ is available for restricted diffusion, even in one

[1] Fax: +81-298-54-4526, E-mail: barzykin@nimc.go.jp.

1090-7807/99 $30.00

dimension. However, the problem is easily handled in the two-pulse scheme within the short gradient pulse limit ($g \to \infty$, $\delta \to 0$, while $q = g\delta$ remains finite). The echo signal is then related to the Green's function $G(\mathbf{r}, \mathbf{r}', t)$ of the diffusion operator as follows (*25*),

$$M_{ST}(\Delta, \mathbf{q}) = \int d\mathbf{r}d\mathbf{r}' m(\mathbf{r}, 0) e^{i\mathbf{q}\cdot(\mathbf{r}-\mathbf{r}')} G(\mathbf{r}, \mathbf{r}', \Delta), \qquad [7]$$

where $m(\mathbf{r}, 0)$ is the initial distribution, typically equilibrium, $m(\mathbf{r}, 0) = \rho(\mathbf{r})$, and the vector $\mathbf{q}$ is directed along the gradient. $G(\mathbf{r}, \mathbf{r}', t)$ satisfies the equation

$$\left(\frac{\partial}{\partial t} - D\nabla^2\right) G(\mathbf{r}, \mathbf{r}', t) = \delta(\mathbf{r} - \mathbf{r}')\delta(t), \qquad [8]$$

and the boundary condition,

$$D\mathbf{n} \cdot \nabla G + HG = 0, \qquad [9]$$

at the interface of the confinement, where $\mathbf{n}$ is the outward surface normal and H is the effective surface relaxivity. $H = 0$ corresponds to the case of perfect reflection which is mathematically special, since only in this case is $G(\mathbf{r}, \mathbf{r}', t)$ conservative and $G(\mathbf{r}, \mathbf{r}', \infty) = \rho(\mathbf{r}')$. The narrow-pulse approximation expressions for the echo signal are available for all the basic geometries (rectangular, cylindrical, and spherical), with both reflecting and relaxing walls (*14, 16, 26–32*). It has been possible to analyze even more complicated geometries (*13*) as well as to study the exchange of material between different confinements (*9–11, 17*) and with the surrounding medium (*33, 34*). A characteristic feature of the short-gradient-pulse experiment is the so-called "diffusive diffraction"—coherence phenomena directly attributable to the underlying structure (*8*).

With modern development in NMR hardware, it has indeed become possible to produce short gradient pulses of high intensity during which the motion due to diffusion is negligible. However, the validity of the narrow-pulse approximation remains one of the central concerns of the gradient NMR community (*27, 28, 32, 35–40*). Practically, the narrow-pulse limit is not always realizable. The need to ensure that the displacement is small during the pulses constrains the distance scales which can be probed using this experiment. Numerical simulations have shown that finite pulse widths may, if not completely destroy the coherence, at least considerably smear and shift the diffraction peaks (*27, 28, 35, 36*). Since there are always other complications in real systems which may cause similar effects, such as the size and shape polydispersity of the confinements, surface relaxation, etc., one has to understand the role of finite pulse widths in a controllable and simple way. Furthermore, there are certain applications where the gradient is constant, as in stray field experiments.

Diffusion during the gradient pulses introduces considerable complications into analytical study. Several approximations are available. One is termed the Gaussian phase approximation in the NMR literature, which is otherwise known as the truncated cumulant expansion. This approximation prevailed until recently (*27, 38, 41–47*). The cumulant expansion result for the echo signal is

$$M(t) = \exp\left[-\frac{1}{2} g^2 \int_0^t dt' \int_0^t dt'' f(t') f(t'') K(t' - t'')\right], \qquad [10]$$

where the correlator is defined as

$$K(t) = \int d\mathbf{r}d\mathbf{r}' xx' \rho(\mathbf{r}) G(\mathbf{r}, \mathbf{r}', t). \qquad [11]$$

Based on the assumption of the Gaussian phase distribution, as in the case of free diffusion, the cumulant expansion has a very narrow range of applicability limited to short times in the steady gradient experiment and to small q in the Stejskal–Tanner experiment. This is where the spins start to "feel" the walls. The cumulant expansion fails to predict oscillations of the signal at high gradient strengths in the steady gradient case and it does not exhibit any diffraction-like minima for the two-pulse gradient profile (*39, 48*).

Sheltraw and Kenkre have introduced the memory-function approximation on the basis of the application of the projection operator method to the evolution equation of the system density matrix (*39*). Their main result,

$$\dot{M}(t) + g^2 f(t) \int_0^t dt' f(t') K(t - t') M(t') = 0, \qquad [12]$$

is derived perturbatively, assuming the gradient to be small and, as a consequence, it does not reproduce the proper narrow-pulse limit. However, qualitatively this technique predicts both the oscillations and the diffraction effects. The memory-function results have an appealing simplicity and are certainly useful in their range of applicability (small g). The cumulant results can be derived from the memory-function results in the Markovian approximation, i.e., by removing $M(t')$ from the integral in Eq. [12].

An alternative and very successful multiple propagator approach has been developed by Caprihan, Wang, and Fukushima (*32*). The method is based on the representation of the general gradient waveform by a succession of sharp impulses with an appropriate propagator for each stage of the evolution. Although the idea is clear and simple, the final expressions are cumbersome and computationally quite intensive. Callaghan

has shown that the multiple propagator scheme can be realized in a matrix form considerably simplifying numerical calculations (*40*). This certainly is a practical solution to the problem at hand for an arbitrary gradient waveform. Can the theory provide any simpler recipe, say, for a steady gradient? This question has been addressed very recently and the answer is yes. We have applied the projection operator method directly to the Bloch–Torrey equation with $f_{SG}(t) = 1$ and obtained an exact nonperturbative solution for the total magnetization in a closed matrix form in terms of the eigenmodes of the diffusion propagator (*48*). The memory-function result is reproduced in the limit of small g. Any step-wise gradient pulse sequence can be treated analytically in the same way since the evolution of the magnetization density between the pulses is purely diffusive and thus known. As an illustrative example, we have considered diffusion on a line segment with perfectly reflecting boundaries, both under a steady gradient and for the Stejskal–Tanner pulse sequence. The purpose of this paper is to derive the corresponding formulas for other basic geometries, i.e., for cylinders and spheres, as well as to include the surface relaxation.

DIRECT SOLUTION IN ONE DIMENSION

Before proceeding further with the matrix solution mentioned in the Introduction, we will show that in one dimension, the exact solution of the Bloch–Torrey equation under a steady gradient, $f_{SG}(t) = 1$, can be obtained directly. Consider diffusion on a line segment of length $2a$. Practically, this means that diffusion is restricted only in one dimension, such as by two parallel planes. The spacing between the planes is denoted as $2a$ rather than a, in order to more directly compare with the case of the cylinder and the sphere. The gradient is applied along the direction normal to the planes. It is convenient to use dimensionless length and time, i.e., $x \to x/a$ and $t \to Dt/a^2$. The only parameter of the problem is now $\zeta = ga^3/D$, which is the ratio of the maximum difference between the precessional frequencies in the confining space ga to the inverse of the characteristic diffusion time D/a^2. The Bloch–Torrey equation takes the form

$$\frac{\partial}{\partial t} m(x, t) = -i\zeta x m(x, t) + \frac{\partial^2}{\partial x^2} m(x, t), \qquad [13]$$

with $x \in [-1, 1]$. The origin is at the center of the segment. After Laplace transformation over time Eq. [13] reduces to the ordinary differential equation

$$\hat{m}''(x, s) - (s + i\zeta x)\hat{m}(x, s) = -m(x, 0), \qquad [14]$$

where

$$\hat{m}(x, s) = \int_0^\infty dt e^{-st} m(x, t) \qquad [15]$$

denotes the transform. The general solution of the above equation is given by

$$\hat{m}(x, s) = C_1 y_1 + C_2 y_2 + y_1 Y_2 - y_2 Y_1, \qquad [16]$$

where C_1 and C_2 are the constants determined by the boundary conditions,

$$y_1 = z^{1/2} I_{1/3}(w), \qquad [17]$$

$$y_2 = z^{1/2} K_{1/3}(w), \qquad [18]$$

with $z = x - is/\zeta$ and $w = \frac{2}{3}(i\zeta)^{1/2} z^{3/2}$, which represent two linearly independent solutions of the corresponding homogeneous equation, and

$$Y_j = \frac{2}{3} \int dx\, y_j\, m(x, 0), \qquad [19]$$

$j = 1, 2$. I_ν and K_ν denote the Bessel functions. For an equilibrium initial distribution, $m(x, 0) = \frac{1}{2}$, we obtain

$$Y_1 = \tfrac{1}{2}(i\zeta)^{-1/2}\Gamma^{-1}\left(\frac{4}{3}\right)\left(\frac{w}{2}\right)^{4/3} {}_1F_2\left(\frac{2}{3}; \frac{4}{3}, \frac{5}{3}; \frac{w^2}{4}\right), \qquad [20]$$

$$Y_2 = \pi(3i\zeta)^{-1/2}\Gamma^{-1}\left(\frac{2}{3}\right)\left(\frac{w}{2}\right)^{2/3} \times {}_1F_2\left(\frac{1}{3}; \frac{2}{3}, \frac{4}{3}; \frac{w^2}{4}\right) - (\pi/2\sqrt{3})Y_1, \qquad [21]$$

where $\Gamma(\nu)$ is the gamma function and ${}_1F_2$ is the hypergeometric function. In order to calculate the signal, we must integrate $\hat{m}(x, s)$ over x and then perform the inverse Laplace transformation. The solution obtained appears to be more of academic interest than of any practical value since it involves rather complicated functions of complex argument making Laplace inversion a tricky numerical procedure which is hardly advantageous over a straightforward numerical integration of the original partial differential equation using a standard finite difference scheme. Besides, the approach itself is not general and applies only for this particular restricted diffusion problem.

MATRIX SOLUTION

Steady Gradient

A general and systematic way to treat the spin-echo problem in restricted geometries is to express the solution in terms of the Green's function of the diffusion operator which contains all the information about the confinement. Thereby we will just reduce one problem to another, of course, but to a considerably simpler one. Methods of solution of the diffusion equation in various geometries are well known (*49*). Some geometries are tractable exactly. In this sense, the spin-echo problem in itself will be solved. We have been able to fulfill this task recently for the case of a steady gradient by using the projection operator technique (*48*). The method is described in full detail elsewhere for a physically different but mathematically equivalent problem of diffusion-assisted reaction kinetics (*50*). By using the standard eigenmode expansion of the Green's function (*49*),

$$G(\mathbf{r}, \mathbf{r}', t) = \rho(\mathbf{r}) \sum_{n=0}^{\infty} u_n(\mathbf{r}) u_n(\mathbf{r}') e^{-\lambda_n t}, \qquad [22]$$

where $u_n(\mathbf{r})$ denote the normalized eigenfunctions and λ_n the associated eigenvalues, we can write the final solution for the total magnetization in the matrix form

$$\hat{M}_{\mathrm{SG}}(s) = [\hat{\mathbf{Q}}^{-1}(s)]_{0,0}, \qquad [23]$$

where

$$\hat{\mathbf{Q}}(s) = s\mathbf{I} + \mathbf{\Lambda} + ig\mathbf{W}, \qquad [24]$$

$$W_{n,n'} = \int d\mathbf{r}\, x\rho(\mathbf{r}) u_n(\mathbf{r}) u_{n'}(\mathbf{r}), \qquad [25]$$

$$\Lambda_{n,n'} = \lambda_n \delta_{n,n'}, \qquad [26]$$

$n, n' = 0, 1, \ldots, \infty$, $\mathbf{I}$ is the identity matrix, and $\delta_{n,n'}$ is the Kronecker delta. The above solution assumes the equilibrium initial condition and the perfectly reflecting boundary condition. Originally, we presented it in a somewhat different, albeit completely equivalent, form obtained naturally from the operator solution with all the operators projected onto the equilibrium distribution.

Equation [23] can be derived without projection operators, just by expanding $m(\mathbf{r}, t)$ in terms of the known basis. This procedure is familiar from quantum mechanics. By substituting the expansion

$$m(\mathbf{r}, t) = \rho(\mathbf{r}) \sum_{n=0}^{\infty} a_n(t) u_n(\mathbf{r}) \qquad [27]$$

into Eq. [1], we obtain for the coefficients,

$$\mathbf{a}(t) = \exp[-t(\mathbf{\Lambda} + ig\mathbf{W})] \cdot \mathbf{a}(0), \qquad [28]$$

where

$$a_n(0) = \int d\mathbf{r} u_n(\mathbf{r}) m(\mathbf{r}, 0). \qquad [29]$$

Given the equilibrium initial condition, we can write for the signal,

$$M_{\mathrm{SG}}(t) = \mathbf{U}^T \cdot \exp[-t(\mathbf{\Lambda} + ig\mathbf{W})] \cdot \mathbf{U}, \qquad [30]$$

or in the Laplace domain,

$$\hat{M}_{\mathrm{SG}}(s) = \mathbf{U}^T \cdot \hat{\mathbf{Q}}^{-1}(s) \cdot \mathbf{U}, \qquad [31]$$

where

$$U_n = \int d\mathbf{r} u_n(\mathbf{r}) \rho(\mathbf{r}). \qquad [32]$$

It should be noted that in an experiment the signal is usually normalized to its amplitude in the absence of the gradient, i.e.,

$$E_{\mathrm{SG}}(t) = \frac{\mathbf{U}^T \cdot \exp[-t(\mathbf{\Lambda} + ig\mathbf{W})] \cdot \mathbf{U}}{\mathbf{U}^T \cdot \exp(-t\mathbf{\Lambda}) \cdot \mathbf{U}}. \qquad [33]$$

In the case of perfectly reflecting boundaries, $u_0(\mathbf{r}) = 1$, $U_n = \delta_{n,0}$, $E_{\mathrm{SG}}(t) = M_{\mathrm{SG}}(t)$, and Eq. [31] reduces to Eq. [23].

The matrix solution was, in fact, implicit in the work of Robertson, who considered the spin-echo restricted-diffusion problem under a steady gradient in one dimension (*42*). However, instead of analyzing this solution, he reformulated the problem in terms of the density matrix, applied the projection operator method, performed the perturbation expansion in powers of ζ, made a local-time approximation, and arrived at the first-order truncated cumulant expansion in the end. We have seen that systematic application of the projection operator method to the Bloch–Torrey equation under a steady gradient leads back to the matrix solution; nothing else can be expected.

The above solution is exact although it contains matrices of infinite dimensions. In practice, we need to truncate the matrices at a certain finite dimension N which should be chosen depending on the gradient strength. Convergence of the solution in this respect is guaranteed by rapidly increasing eigenvalues. This is very important. Fast convergence is the key factor of the applicability of this method. We have shown that, at least in the case of one-dimensional restriction, only a few modes are required to attain excellent accuracy of the truncated

matrix solution for experimentally typical values of the gradient strength (*48*).

Numerically, after the matrices $\mathbf{\Lambda}$ and $\mathbf{W}$ are defined, one can simply evaluate the matrix exponential in Eq. [30] to find the signal. Analytically, the structure of the truncated matrix solution can be more clearly demonstrated by Laplace-inverting Eq. [31]. The evolution of the total magnetization is then described by a superposition of N exponentials in the time domain,

$$M_{\mathrm{SG}}(t) = \sum_{j=1}^{N} c_j \exp(s_j t), \qquad [34]$$

where s_j are the roots of $\Delta(s) = 0$, $\Delta(s)$ is the determinant of $\hat{\mathbf{Q}}(s)$. Note that $\mathrm{Re}(s_j) < 0$. The coefficients are given by

$$c_j = \frac{\mathbf{U}^T \cdot \tilde{\mathbf{Q}}(s_j) \cdot \mathbf{U}}{\Delta_j(s_j)}, \qquad [35]$$

where $\tilde{\mathbf{Q}}(s)$ is the adjoint matrix of $\hat{\mathbf{Q}}(s)$, and

$$\Delta_j(s) = \frac{\Delta(s)}{s - s_j}. \qquad [36]$$

In the case of perfectly reflecting boundaries,

$$c_j = \mu_{0,0}(s_j)\Delta_j^{-1}(s_j), \qquad [37]$$

where $\mu_{0,0}(s)$ is the minor of $\hat{Q}_{0,0}(s)$.

Thus, the signal relaxation modes are determined by the roots of the Nth-order polynomial. The two-mode approximation essentially coincides with the predictions of the memory-function theory. Particularly simple expression is obtained for the basic geometries discussed below (parallel planes, cylinder, and sphere). As a consequence of the gradient linearity and the symmetry of these simple geometries, we have $\rho(\mathbf{r}) = \rho$ and $W_{0,0} = W_{1,1} = U_1 = 0$. We also have

$$W_{0,1} = W_{1,0} = \rho \int d\mathbf{r}\, x u_0(\mathbf{r}) u_1(\mathbf{r}), \qquad [38]$$

so that

$$\Delta(s) = (s + \lambda_0)(s + \lambda_1) + \epsilon^2, \qquad [39]$$

where $\epsilon = gW_{0,1}$, and finally for the echo signal,

$$M_{\mathrm{SG}}^{(2)}(t) = U_0^2 e^{-\lambda_0 t} e^{-\gamma t}\left[\cosh(\omega t) + \frac{\gamma}{\omega}\sinh(\omega t)\right], \qquad [40]$$

where

$$\gamma = \tfrac{1}{2}(\lambda_1 - \lambda_0), \qquad [41]$$

$$\omega = (\gamma^2 - \epsilon^2)^{1/2}. \qquad [42]$$

The normalized echo signal is given by

$$E_{\mathrm{SG}}^{(2)}(t) = e^{-\gamma t}\left[\cosh(\omega t) + \frac{\gamma}{\omega}\sinh(\omega t)\right], \qquad [43]$$

This generalizes the memory-function result of Sheltraw and Kenkre derived for perfectly reflecting boundaries (*39*). Inclusion of additional eigenmodes does not essentially improve the memory-function solution. In contrast, the truncated matrix solution rapidly converges to the exact result as the number of modes is increased.

Previously, we used a slightly different terminology. By the N-mode approximation we meant that N lowest eigenmodes are involved *besides* the equilibrium mode. We feel that all the modes should be included in the definition, particularly in view of the fact that in the case of surface relaxation there is no equilibrium.

Stejskal–Tanner Pulse Sequence

Now that we understand how to handle the steady gradient case, we can focus on the experimentally more important Stejskal–Tanner pulse sequence. Our goal is the signal at the end of the second pulse. It does not change after the gradient is switched off in the case of perfectly reflecting boundaries since the bulk relaxation is factored out. We will consider this case first and then discuss the effect of surface relaxation.

We have three consecutive stages. The magnetization density at the end of one stage provides the initial condition for the subsequent stage. Using the results of the preceding section we can write for the magnetization density after the first gradient pulse,

$$m(\mathbf{r}, \delta) = \rho(\mathbf{r})\mathbf{u}^T(\mathbf{r}) \cdot e^{-\delta \mathbf{V}^*} \cdot \mathbf{U}, \qquad [44]$$

where $\mathbf{V} = \mathbf{\Lambda} + ig\mathbf{W}$ and the asterisk denotes the complex conjugate. The intermediate stage is purely diffusive and thus

$$m(\mathbf{r}, \Delta) = \int d\mathbf{r}'\, G(\mathbf{r}, \mathbf{r}', \Delta - \delta) m(\mathbf{r}', \delta) \qquad [45]$$

$$= \rho(\mathbf{r})\mathbf{u}^T(\mathbf{r}) \cdot e^{-(\Delta-\delta)\mathbf{\Lambda}} \cdot e^{-\delta \mathbf{V}^*} \cdot \mathbf{U}.$$

Given this initial condition, the magnetization density at the end of the second pulse is given by

$$m(\mathbf{r},\,\Delta+\delta)=\rho(\mathbf{r})\mathbf{u}^T(\mathbf{r})\cdot e^{-\delta\mathbf{V}}\cdot e^{-(\Delta-\delta)\mathbf{\Lambda}}\cdot e^{-\delta\mathbf{V}^*}\cdot\mathbf{U}. \quad [46]$$

Finally, for the echo signal,

$$M_{\mathrm{ST}}(\Delta,\,\delta)=\mathbf{U}^T\cdot e^{-\delta\mathbf{V}}\cdot e^{-(\Delta-\delta)\mathbf{\Lambda}}\cdot e^{-\delta\mathbf{V}^*}\cdot\mathbf{U}, \quad [47]$$

and taking into account the fact that $U_n=\delta_{n,0}$ for perfectly reflecting boundaries,

$$M_{\mathrm{ST}}(\Delta,\,\delta)=[e^{-\delta\mathbf{V}}\cdot e^{-(\Delta-\delta)\mathbf{\Lambda}}\cdot e^{-\delta\mathbf{V}^*}]_{0,0}. \quad [48]$$

In the long-time limit ($\Delta\to\infty$) this reduces to

$$M_{\mathrm{ST}}(\infty,\,\delta)=M_{\mathrm{SG}}(\delta)M^*_{\mathrm{SG}}(\delta). \quad [49]$$

Due to the symmetry of the geometries we consider here, $M^*_{\mathrm{SG}}(\delta)=M_{\mathrm{SG}}(\delta)$, but this is not true in general. The truncated matrix solution can be handled either by numerically evaluating the matrix exponentials in Eq. [48] or by expressing the signal in the form

$$M_{\mathrm{ST}}(\Delta,\,\delta)=\sum_{k,l=1}^{N}c_{kl}\,e^{(s_l+\sigma_k)\delta}, \quad [50]$$

where

$$c_{kl}=\sum_{j=0}^{N-1}\frac{\mu_{0,j}(s_l)\mu^*_{j,0}(\sigma_k)}{\Delta_l(s_l)\Delta^*_k(\sigma_k)}\,e^{-(\Delta-\delta)\lambda_j} \quad [51]$$

and σ_k are the roots of $\Delta^*(\sigma)=0$. For the high symmetry problems considered here, $\sigma_k=s_k$.

In the case of relaxing walls we can still use Eq. [47] to calculate the total magnetization provided that the first gradient pulse comes immediately after the first RF pulse and the signal is acquired immediately after the second gradient pulse, i.e., $\Delta+\delta=2\tau_{\mathrm{RF}}$, where τ_{RF} is the RF pulse separation in the Hahn spin-echo pulse sequence. Otherwise, we must take into account the distortion of the equilibrium magnetization density distribution before the first gradient pulse and the additional signal relaxation after the second. The result is

$$M_{\mathrm{ST}}(\Delta,\,\delta,\,t_1,\,t_2)=\mathbf{U}^T\cdot e^{-t_1\mathbf{\Lambda}}\cdot e^{-\delta\mathbf{V}}\cdot e^{-(\Delta-\delta)\mathbf{\Lambda}}\cdot e^{-\delta\mathbf{V}^*}\cdot e^{-t_2\mathbf{\Lambda}}\cdot\mathbf{U}, \quad [52]$$

where $t_2=2\tau_{\mathrm{RF}}-t_1-\Delta-\delta$ (see Fig. 1). Equation [50] can still be used but the coefficients are now given by

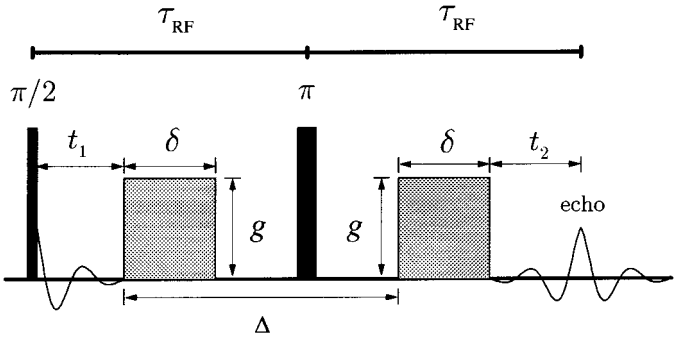

FIG. 1. Schematic representation of the Stejskal–Tanner pulsed-gradient spin-echo experiment.

$$c_{kl}=\frac{\mathbf{U}^T\cdot e^{-t_1\mathbf{\Lambda}}\cdot\tilde{\mathbf{Q}}(s_l)\cdot e^{-(\Delta-\delta)\mathbf{\Lambda}}\cdot\tilde{\mathbf{Q}}^*(\sigma_k)\cdot e^{-t_2\mathbf{\Lambda}}\cdot\mathbf{U}}{\Delta_l(s_l)\Delta^*_k(\sigma_k)}. \quad [53]$$

The normalized echo signal,

$$E_{\mathrm{ST}}(\Delta,\,\delta,\,t_1,\,t_2)=\frac{M_{\mathrm{ST}}(\Delta,\,\delta,\,t_1,\,t_2)}{\mathbf{U}^T\cdot e^{-2\tau\mathbf{\Lambda}}\cdot\mathbf{U}}, \quad [54]$$

is experimentally observable.

The above general expressions are considerably simplified within the two-mode approximation for the basic geometries discussed below. We obtain

$$E^{(2)}_{\mathrm{ST}}(\Delta,\,\delta)=[E^{(2)}_{\mathrm{SG}}(\delta)]^2+(\epsilon/\omega)^2\sinh^2(\omega\delta)e^{-2\gamma\Delta}, \quad [55]$$

irrespective of t_1 and t_2. This generalizes the memory-function result of Sheltraw and Kenkre derived for perfectly reflecting boundaries (*39*). We can include more modes, if necessary, to attain any prescribed precision. It is also clear that we can consider any step-wise pulse sequence in the same way.

MATRIX ELEMENTS

Rectangular Geometry

We now focus on the application of the above general results to the simplest geometries with one-, two-, and three-dimensional restrictions. We begin with a one-dimensional problem in which diffusion occurs between a pair of parallel planes and the gradient is applied along the direction normal to the planes. In dimensionless form, this problem is described by Eq. [13]. We have $\rho(x)=\frac{1}{2}$ and for the eigenmodes,

$$\lambda_n=\alpha_n^2, \quad [56]$$

$$u_n(x)=\sqrt{2}\beta_n\left(\cos[\alpha_n(x+1)]+\frac{h}{\alpha_n}\sin[\alpha_n(x+1)]\right), \quad [57]$$

where

$$\beta_n = \frac{\alpha_n}{\sqrt{\alpha_n^2 + h(h+1)}}, \quad [58]$$

$h = Ha/D$, and α_n are positive roots of the equation

$$\tan(2\alpha_n) = \frac{2h\alpha_n}{\alpha_n^2 - h^2}, \quad [59]$$

numbered in increasing order, $n = 0, 1, \ldots, \infty$. As a result, we have for the non-zero elements of the **W**-matrix,

$$W_{2j,2k+1} = W_{2k+1,2j} = -2\beta_{2j}\beta_{2k+1}\frac{\alpha_{2j}^2 + \alpha_{2k+1}^2 + 2h^2}{(\alpha_{2j}^2 - \alpha_{2k+1}^2)^2}, \quad [60]$$

where $j, k = 0, 1, \ldots, \infty$. Note that even and odd roots actually satisfy different equations,

$$\alpha_{2j}\tan(\alpha_{2j}) = h, \quad [61]$$

$$\alpha_{2j+1}\cot(\alpha_{2j+1}) = -h. \quad [62]$$

It can be readily shown that in the limit of $h \to 0$,

$$\alpha_n = \pi n/2, \quad [63]$$

$$u_n(x) = (2 - \delta_{n,0})^{1/2}\cos[\alpha_n(x+1)], \quad [64]$$

and the result for perfectly reflecting walls is reproduced,

$$W_{2j,2k+1} = W_{2k+1,2j} = -\pi^{-2}(1 + \delta_{j,0})^{-1/2} \times [(j + k + \tfrac{1}{2})^{-2} + (j - k - \tfrac{1}{2})^{-2}]. \quad [65]$$

We also need to define the vector **U**,

$$U_{2j} = \sqrt{2}h\alpha_{2j}^{-1}[\alpha_{2j}^2 + h(h+1)]^{-1/2}. \quad [66]$$

Odd elements are zero. As mentioned in the preceding section, $U_n = \delta_{n,0}$ for perfectly reflecting boundaries.

Cylindrical Geometry

This is a two-dimensional problem handled in polar coordinates, r and θ. The gradient is applied across the diameter. Again, we use dimensionless distance, $r \to r/a$, time, $t \to Dt/a^2$, and the surface relaxivity, $h = Ha/D$, where a is the radius of the cylinder. We have $\rho(\mathbf{r}) = 1/\pi$ and for the eigenmodes,

$$\lambda_{nm} = \alpha_{nm}^2, \quad [67]$$

$$u_{nm}(\mathbf{r}) = (2 - \delta_{n,0})^{1/2}\beta_{nm}J_n(\alpha_{nm}r)\cos(n\theta), \quad [68]$$

where J_n are the Bessel functions,

$$\beta_{nm} = \frac{\alpha_{nm}}{J_n(\alpha_{nm})}(\alpha_{nm}^2 + h^2 - n^2)^{-1/2}, \quad [69]$$

and α_{nm} are the roots of

$$\alpha_{nm}J_n'(\alpha_{nm})/J_n(\alpha_{nm}) = -h, \quad [70]$$

numbered in increasing order, $n, m = 0, 1, \ldots, \infty$. In the limit of $h \to 0$, the lowest root tends to zero, $\alpha_{00} \simeq \sqrt{2h} \to 0$, corresponding to the equilibrium distribution, $u_{00}(\mathbf{r}) = 1$. It is convenient to keep double indices here. In practice, we need to place all the elements in order of increasing α_{nm}.

The elements of the **W**-matrix are given by

$$W_{nm,n'm'} = \delta_{n,n'\pm1}(1 + \delta_{n,0} + \delta_{n',0})^{1/2}\beta_{nm}\beta_{n'm'} \times \int_0^1 dr\, r^2 J_n(\alpha_{nm}r)J_{n'}(\alpha_{n'm'}r). \quad [71]$$

We could not find any simple analytical representation for the integral in Eq. [71]. Numerical integration is trivial, however. In the case of perfectly reflecting boundaries, we obtain for the elements of **W** which characterize the correlation between the equilibrium mode and the higher eigenmodes,

$$W_{00,1m} = \sqrt{2}\alpha_{1m}^{-1}(\alpha_{1m}^2 - 1)^{-1/2}. \quad [72]$$

Only these correlation factors appear in the memory-function and the first-order truncated-cumulant-expansion solutions. Finally, we have for the non-zero elements of **U**,

$$U_{0m} = 2h\alpha_{0m}^{-1}(\alpha_{0m}^2 + h^2)^{-1/2}. \quad [73]$$

Spherical Geometry

For a sphere of radius a, the gradient is applied along the polar axis of the spherical polar coordinate frame. We use the same dimensionless parameters as those above. We have $\rho(\mathbf{r}) = 3/(4\pi)$ and for the eigenfunctions,

$$u_{nm}(\mathbf{r}) = \sqrt{2/3}\beta_{nm}j_n(\alpha_{nm}r)P_n(\cos\theta), \quad [74]$$

where j_n are the spherical Bessel functions, P_n are the Legendre polynomials, and

$$\beta_{nm}^2 = \frac{2n+1}{h(h-1)+\alpha_{nm}^2 - n(n+1)} \frac{\alpha_{nm}^2}{j_n^2(\alpha_{nm})}. \quad [75]$$

The eigenvalues are given by $\lambda_{nm} = \alpha_{nm}^2$, as above, but now α_{nm} are the roots of

$$\alpha_{nm} j_n'(\alpha_{nm})/j_n(\alpha_{nm}) = -h, \quad [76]$$

numbered in increasing order. Everything is very similar to the cylinder case. In the limit of $h \to 0$, the lowest root tends to zero, $\alpha_{00} \simeq \sqrt{3h} \to 0$, corresponding to the equilibrium distribution, $u_{00}(\mathbf{r}) = 1$. The **W**-matrix elements are given by

$$W_{nm,n'm'} = \delta_{n,n'\pm 1} \frac{2(n_< + 1)}{(2n_< + 1)(2n_< + 3)} \times \beta_{nm}\beta_{n'm'} \int_0^1 dr r^3 j_n(\alpha_{nm} r) j_{n'}(\alpha_{n'm'} r), \quad [77]$$

where $n_< = \min(n, n')$. Integration over r in Eq. [77] can be performed analytically but the results are too cumbersome to offer any practical advantage over the straightforward numerical integration. We only present the elements responsible for the correlation between the equilibrium mode and the higher eigenmodes in the case of perfectly reflecting walls,

$$W_{00,1m} = \sqrt{2}\alpha_{1m}^{-1}(\alpha_{1m}^2 - 2)^{-1/2}. \quad [78]$$

Only these correlation factors appear in the memory-function and the first-order truncated-cumulant-expansion solutions. Finally, we have for the non-zero elements of **U**,

$$U_{0m} = \sqrt{6h}\alpha_{0m}^{-1}[\alpha_{0m}^2 + h(h-1)]^{-1/2}. \quad [79]$$

NUMERICAL RESULTS

Now that the matrices **Λ**, **W**, and **U** are defined, the rest is a technical matter. Since the effects of surface relaxation and finite pulse widths have been analyzed in sufficient detail in the literature (*27–29, 32, 35–40*), here we shall only demonstrate the convergence of the truncated matrix solution for a typical set of parameter values. Figure 2 shows the time evolution of the normalized total magnetization under a steady gradient, $E_{SG}(t)$, in different geometries for $h = 0.5$ and $\zeta = 30$. This is a rather large value of ζ (i.e., the gradient strength), resulting in strong oscillations. Note that the Gaussian phase approximation is completely inadequate here (*39, 48*). The two-mode approximation describes well the initial stage of the kinetics but fails at long times. The three-mode approximation is much better and for $N > 5$ the curves become practically indistinguishable. The numerical solution of the Bloch–Torrey equation obtained via a standard discretization procedure in the one-dimensional case is also shown for comparison. The agreement is perfect.

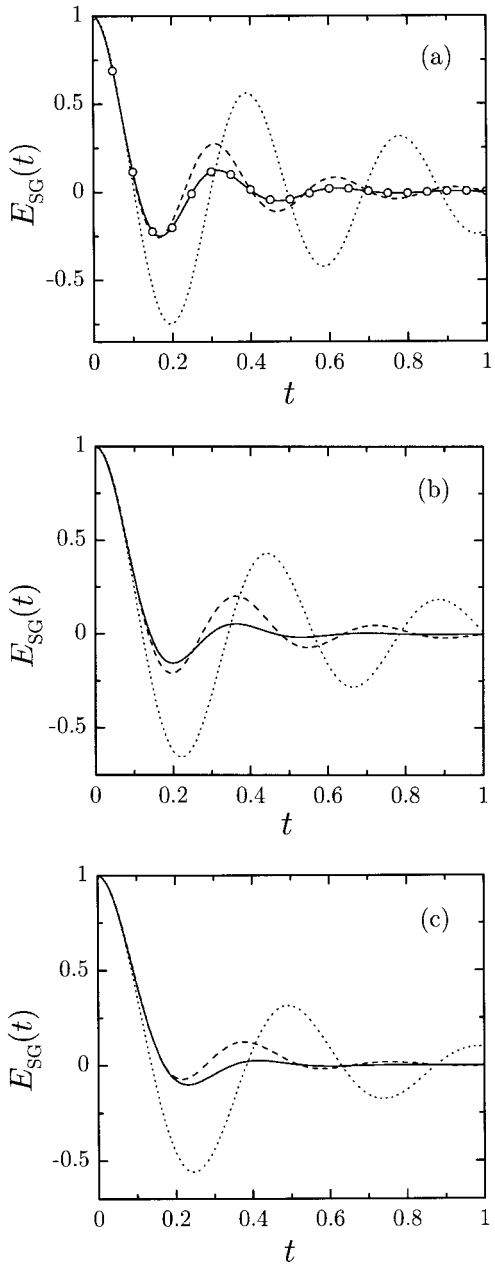

FIG. 2. Time evolution of the normalized magnetization under a steady gradient, $E_{SG}(t)$, for spins diffusing between planes (a), in a cylinder (b), and in a sphere (c), with $h = 0.5$ and $\zeta = 30$ (dimensionless parameters defined in the text). The curves correspond to the N-mode truncated matrix solution with $N = 2$ (dotted), $N = 3$ (dashed), $N = 6$ (solid), and the short-gradient-pulse approximation (dash–dotted). Circles represent the numerical solution of the Bloch–Torrey equation in the one-dimensional case.

Figure 3 illustrates the normalized echo signal for the Stejskal–Tanner pulse sequence, $E_{ST}(\Delta, \delta)$, as a function of

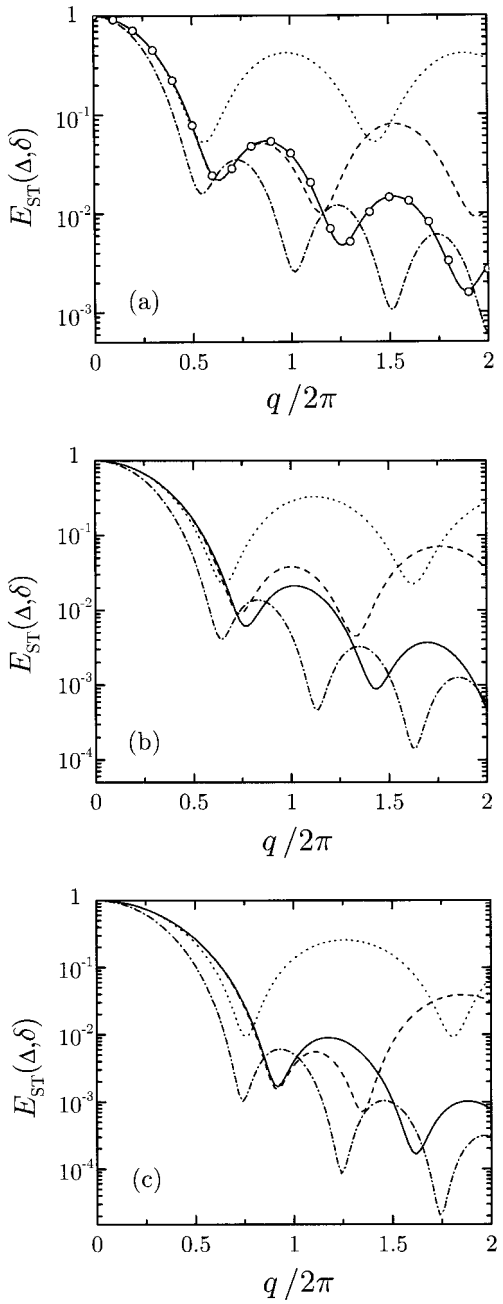

FIG. 3. Normalized echo signal as a function of the amplitude of the reduced wavevector $q/2\pi$ for the Stejskal–Tanner pulse sequence, $E_{ST}(\Delta, \delta)$, for spins diffusing between planes (a), in a cylinder (b), and in a sphere (c), with $h = 0.5$, $\delta = 0.3$, $\Delta = 1$, and $t_1 = t_2 = 0$ (dimensionless parameters defined in the text). The curves correspond to the N-mode truncated matrix solution with $N = 2$ (dotted), $N = 3$ (dashed), $N = 8$ (solid), and the short-gradient-pulse approximation (dash–dotted). Circles represent the numerical solution of the Bloch–Torrey equation in the one-dimensional case.

$q = \zeta\delta$ in different geometries for $h = 0.5$, $\delta = 0.3$, and $\Delta = 1$. The two-mode approximation works well for small q and can be used to determine the apparent diffusion coefficient. For one-dimensional restricted diffusion, convergence of the truncated matrix solution is achieved within five modes. The numerical solution is also presented in this case and the agreement is again perfect. For cylinders and spheres, more modes are required but still for $N > 7$ the curves are practically indistinguishable within the range of q displayed. The convergence is better for smaller surface relaxivity and for larger pulse separation. We are talking about the absolute convergence here. Noting the log scale in Fig. 3 we can see that deviations of the N-mode predictions from the exact results will be within the experimental error even for $N \geq 3$, particularly in view of the fact that we are dealing with the normalized echo signal. In fact, experimentalists are sometimes satisfied with the accuracy of the Gaussian phase approximation (*27*), which is always worse than even that of the two-mode approximation.

The short-gradient-pulse approximation is also shown in Fig. 3 for comparison. The corresponding expressions can be found in the literature (*29*). Here we only present the result for the planes, which, we believe, is simpler than previously reported, albeit completely equivalent,

$$M_{ST}(\Delta, q) = \frac{1}{2}\sum_{n=0}^{\infty}\frac{[\mathrm{sinc}(\alpha_n + q) + (-1)^n\mathrm{sinc}(\alpha_n - q)]^2}{1 + (-1)^n\mathrm{sinc}(2\alpha_n)}\, e^{-\alpha_n^2\Delta}, \quad [80]$$

where $\mathrm{sinc}(x) = \sin(x)/x$.

Now we show in Fig. 4 the comparison of the predictions of our matrix solution with the simulations by Linse and Söderman (*36*). The parameters chosen correspond to those used in their Figs. 4(c), 5(a), and 6(a), namely, $\Delta^* = D\Delta/(2a)^2 = 0.2$ and $\gamma^* g^* = g(2a)^3/D = 200$. The agreement is excellent. Note that in their definition of the dimensionless parameters the diameter, $2a$, is used instead of the radius, a, as in this work. Also, these authors performed their analysis of the dependence of the echo attenuation on q by keeping the gradient amplitude, g, constant and varying the duration of the gradient pulse, δ. The results shown in Fig. 3 were obtained following a different scheme, where g is varied while δ is kept constant. Both approaches are used in practice.

Finally, the effect of distortion of the equilibrium magnetization density distribution before the first gradient pulse and the additional signal relaxation after the second is illustrated in Fig. 5 for $h = 1$, $\delta = 0.1$, $\Delta = 0.5$, and $t_1 = t_2 = 0.2$ in the one-dimensional case. Although the effect appears to be rather weak, it will be stronger for asymmetric geometries. Thus, to avoid complications, the experiment should be designed in such a way that t_1 and t_2 are as small as possible.

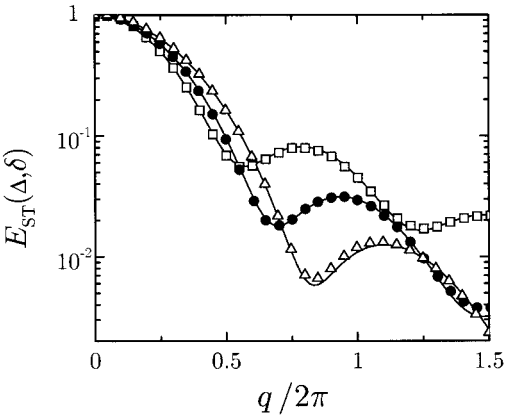

FIG. 4. Comparison of the matrix solution (lines) with the simulation results (symbols) of Linse and Söderman (*36*) for the normalized echo signal as a function of the amplitude of the reduced wavevector $q/2\pi$ for the Stejskal–Tanner pulse sequence, $E_{ST}(\Delta, \delta)$, for spins diffusing between planes (squares), in a cylinder (circles), and in a sphere (triangles) with reflecting walls ($h = 0$), for $\Delta = 0.8$ and $\zeta = 25$ (corresponding to $\Delta^* = 0.2$ and $\gamma^* g^* = 200$ in the notations of Linse and Söderman).

MULTIPLE PROPAGATOR VERSUS STEP-WISE GRADIENT APPROACH

As mentioned in the Introduction, the problem of spin diffusion in restricted geometries under an arbitrary gradient waveform can be handled within the multiple propagator scheme of Caprihan, Wang, and Fukushima (*32*). It is important to establish the relationship between this general method and our matrix solution for a step-wise gradient. As we shall see, this relationship is very simple although the two approaches are based on seemingly different grounds.

The idea of the multiple propagator approach originates from the short-gradient-pulse approximation. The gradient waveform is represented by a succession of δ-function impulses,

$$f_\delta(t) = \tau \sum_{j=0}^{N} c_j \delta(t - j\tau). \qquad [81]$$

It may be convenient to discretize the waveform amplitudes c_j as well, but it is not necessary here and we can simply put $c_j = f(j\tau)$. Thus, the translational motion of spins is subdivided into a sequence of N time intervals τ during which the space evolution of the magnetization density is described by the diffusion propagator, $G(\mathbf{r}, \mathbf{r}', t)$, while all spin phase evolution takes place at well-defined times at the boundaries of those intervals with corresponding phase factors $\exp(-i\mathbf{q}_j \cdot \mathbf{r})$, where $q_j = |\mathbf{q}_j| = g\tau c_j$.

Callaghan has shown (*40*) that such a time discretization procedure leads to a closed matrix form of solution for the total magnetization at the end of the pulse sequence,

$$M(N\tau) = \mathbf{S}^T(\mathbf{q}_0) \cdot \prod_{j=1}^{N-1} [\mathbf{R} \cdot \mathbf{A}(\mathbf{q}_j)] \cdot \mathbf{S}(\mathbf{q}_N), \qquad [82]$$

where

$$S_n(\mathbf{q}) = \int d\mathbf{r} \rho(\mathbf{r}) u_n(\mathbf{r}) \exp(-i\mathbf{q} \cdot \mathbf{r}), \qquad [83]$$

$$A_{n,n'}(\mathbf{q}) = \int d\mathbf{r} \rho(\mathbf{r}) u_n(\mathbf{r}) u_{n'}(\mathbf{r}) \exp(-i\mathbf{q} \cdot \mathbf{r}), \qquad [84]$$

$$\mathbf{R} = \exp(-\tau\mathbf{\Lambda}). \qquad [85]$$

In the case of a steady gradient, $f(t) = 1$, one obtains

$$M_{SG}(N\tau) = \mathbf{S}^T(\mathbf{q}) \cdot [\mathbf{R} \cdot \mathbf{A}(\mathbf{q})]^{N-1} \cdot \mathbf{S}(\mathbf{q}), \qquad [86]$$

where $q = g\tau$. Let us now take the limit $N \to \infty$ with $N\tau = t$. We have

$$\lim_{N\to\infty} \mathbf{S}(\mathbf{q}) = \mathbf{U}, \qquad [87]$$

$\mathbf{R} \cdot A(\mathbf{q}) \simeq \mathbf{I} - \frac{1}{N} t(\mathbf{\Lambda} + ig\mathbf{W})$ and thus

$$\lim_{N\to\infty} [\mathbf{R} \cdot \mathbf{A}(\mathbf{q})]^{N-1} = \exp[-t(\mathbf{\Lambda} + ig\mathbf{W})], \qquad [88]$$

where the matrices $\mathbf{U}$ and $\mathbf{W}$ are defined by Eqs. [32] and [25], respectively. Finally,

$$M_{SG}(t) = \mathbf{U}^T \cdot \exp[-t(\mathbf{\Lambda} + ig\mathbf{W})] \cdot \mathbf{U}; \qquad [89]$$

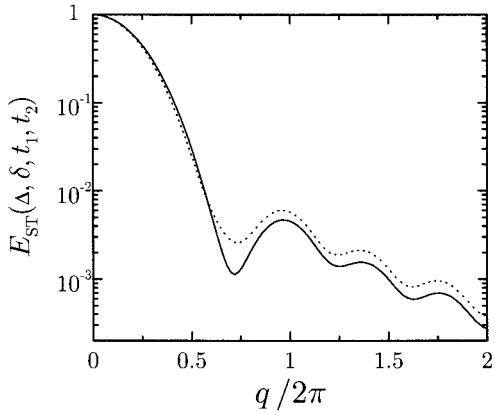

FIG. 5. Normalized echo signal as a function of the amplitude of the reduced wavevector $q/2\pi$ for the Stejskal–Tanner pulse sequence, $E_{ST}(\Delta, \delta, t_1, t_2)$, for spins diffusing between planes. The curves correspond to the following sets of parameters: $h = 1$, $\delta = 0.1$, $\Delta = 0.5$, and $t_1 = t_2 = 0$ (dotted), or $t_1 = t_2 = 0.2$ (solid).

i.e., our matrix solution is reproduced from Callaghan's matrix solution in the continuum limit where the number of sharp gradient impulses in the discrete waveform becomes effectively infinite.

On the other hand, if we assume that the true short-gradient-pulse limit can be reached, at least theoretically, the multiple propagator approach becomes exact while our matrix solution requires effectively an infinite number of diffusion eigenmodes to converge. Let us illustrate this point by considering a single δ-function pulse. The corresponding expression for the total magnetization is

$$M_\delta(\mathbf{q}) = \int d\mathbf{r}\rho(\mathbf{r})\exp(-i\mathbf{q}\cdot\mathbf{r}). \quad [90]$$

In the short-gradient-pulse limit our matrix solution reduces to

$$M_\delta(\mathbf{q}) = \mathbf{U}^T\cdot\exp(-iq\mathbf{W})\cdot\mathbf{U}. \quad [91]$$

Equivalence of the two expressions can be proved by expanding $\exp(-iq\mathbf{W})$ in Eq. [91] in a Taylor series, using the orthogonality condition,

$$\rho(\mathbf{r})\sum_{n=0}^{\infty} u_n(\mathbf{r})u_n(\mathbf{r}') = \delta(\mathbf{r}-\mathbf{r}'), \quad [92]$$

and then collecting the terms back into an exponential form. Analytically, we need an infinite number of eigenmodes to reproduce Eq. [90]. The accuracy of the truncated matrix solution is determined by the amplitude q of the gradient. In other words, the two methods may have their advantages from a practical viewpoint but theoretically they are equivalent, as they should be.

Finally, let us show how to handle an arbitrary waveform within the step-wise gradient approach. In analogy to the multiple propagator scheme, we discretize the waveform,

$$f_\theta(t) = \tau\sum_{j=1}^{N} c_j\,[\theta(t-(j-1)\tau) - \theta(t-j\tau)]. \quad [93]$$

Now step functions are used instead of δ-functions. The amplitudes c_j are chosen in such a way that the area under $f_\theta(t)$ is equal to the area under $f(t)$ for each τ step, i.e.,

$$c_j = \frac{1}{\tau}\int_{(j-1)\tau}^{j\tau} dt\, f(t) \approx \frac{1}{2}\,[\,f((j-1)\tau) + f(j\tau)]. \quad [94]$$

The approximate equality holds for smooth gradient waveforms and small τ. The discretization procedure is illustrated in Fig. 6. As a result, we obtain for the total magnetization at the end of the pulse sequence,

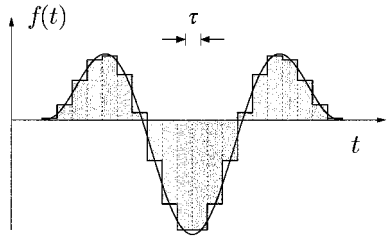

FIG. 6. Step-wise discretization procedure for an arbitrary gradient waveform.

$$M(N\tau) = \mathbf{U}^T\cdot\prod_{j=1}^{N}\exp[-\tau(\mathbf{\Lambda} + igc_j\mathbf{W})]\cdot\mathbf{U}. \quad [95]$$

Thus, any waveform may be handled in a simple and general fashion in terms of just three matrices, **U**, **Λ**, and **W**.

CONCLUDING REMARKS

We have addressed the problem of spin echo in restricted geometries under a step-wise gradient pulse sequence. It has been shown that the evolution of the magnetization density during each pulse can be described in a simple matrix form where the matrices are defined in terms of the eigenmodes of the diffusion operator in the given geometry with appropriate boundary conditions (perfectly reflecting or relaxing walls). Although matrices of infinite dimensions are involved, they can be truncated at a certain finite dimension to attain any prescribed precision. Convergence of the truncated matrix solution is guaranteed by rapidly increasing eigenvalues. Only a few modes are often sufficient to attain excellent accuracy for experimentally typical values of the gradient strength. We have derived simple analytical expressions within the two-mode approximation in the case of relaxing boundaries generalizing previously reported memory-function results. The matrix elements for three basic restricted geometries, namely, a line segment, a cylinder, and a sphere, have been calculated and the behavior of the total magnetization in these cases has been analyzed for the steady gradient as a function of time and for the Stejskal–Tanner pulse sequence as a function of the amplitude of the reduced wavevector. The agreement of the matrix solution with the results of numerical simulations is perfect. We have also established the relationship between our matrix solution and the multiple propagator approach devised to handle arbitrary gradient waveforms by decomposing the waveform into a succession of sharp (δ-function) impulses. A step-wise gradient discretization procedure that offers an alternative simple method for dealing with generalized gradient waveforms has been suggested.

The method of solution of the Bloch–Torrey equation employed here is familiar from quantum mechanics. We have simply shown that given a discrete spectrum of eigenvalues, characteristic of confined systems, this method provides a straightforward way to calculate the echo signal. We believe that at this stage we may say that the problem of spin echo in restricted geometries is solved. This is, of course, in the sense that it is reduced to a simpler restricted diffusion problem. Provided that one can obtain an eigenmode expansion for the diffusion propagator, the solution for the echo may be written down directly, avoiding the need for numerical simulations. For arbitrary gradient waveforms, one can use either the multiple propagator scheme in Callaghan's matrix formulation or the step-wise gradient matrix approach given in this paper. There is no longer any need to resort to the Gaussian phase approximation with its narrow range of applicability. More accurate but equally simple analytical expressions can be obtained within the memory-function approximation (or the two-mode approximation).

ACKNOWLEDGMENT

I thank Dr. W. S. Price for stimulating my interest in the gradient NMR problems.

REFERENCES

1. P. Stilbs, *Prog. NMR Spectrosc.* **19,** 1 (1987).
2. P. T. Callaghan, "Principles of Nuclear Magnetic Resonance Microscopy," Oxford Univ. Press, Oxford (1991).
3. O. Söderman and P. Stilbs, *Prog. NMR Spectrosc.* **26,** 445 (1994).
4. W. S. Price, Gradient NMR, *in* "Annual Reports on NMR Spectroscopy" (G. A. Webb, Ed.), pp. 51–142, Academic Press, London (1996).
5. I. Lönnqvist, A. Khan, and O. Söderman, *J. Colloid Interface Sci.* **144,** 401 (1991).
6. B. Balinov, P. Linse, and O. Söderman, *J. Colloid Interface Sci.* **182,** 539 (1996).
7. M. Schönhoff and O. Söderman, *J. Phys. Chem. B* **101,** 8237 (1997).
8. P. T. Callaghan, A. Coy, D. MacGowan, K. J. Packer, and F. O. Zelaya, *Nature* **351,** 467 (1991).
9. P. T. Callaghan, A. Coy, T. P. J. Halpin, D. MacGowan, K. J. Packer, and F. O. Zelaya, *J. Chem. Phys.* **97,** 651 (1992).
10. D. J. Bergman and K.-J. Dunn, *Phys. Rev. B* **50,** 9153 (1994).
11. K.-J. Dunn and D. J. Bergman, *J. Chem. Phys.* **102,** 3041 (1995).
12. M. D. Hürlimann, K. G. Helmer, L. L. Latour, and C. H. Sotak, *J. Magn. Reson. A* **111,** 169 (1994).
13. P. P. Mitra, P. N. Sen, L. M. Schwartz, and P. L. Doussal, *Phys. Rev. Lett.* **68,** 3555 (1992).
14. P. P. Mitra and P. N. Sen, *Phys. Rev. B* **45,** 143 (1992).
15. P. P. Mitra and P. N. Sen, *Physica A* **186,** 109 (1992).
16. P. P. Mitra, P. N. Sen, and L. M. Schwartz, *Phys. Rev. B* **47,** 8565 (1993).
17. P. N. Sen, L. M. Schwartz, P. P. Mitra, and B. I. Halperin, *Phys. Rev. B* **49,** 215 (1994).
18. K. R. Brownstein and C. E. Tarr, *Phys. Rev. A* **19,** 2446 (1979).
19. W. S. Price and P. W. Kuchel, *J. Magn. Reson.* **90,** 100 (1990).
20. S. R. Wassall, *Biophys. J.* **71,** 2724 (1996).
21. P. W. Kuchel, A. Coy, and P. Stilbs, *Magn. Reson. Med.* **37,** 637 (1997).
22. H. C. Torrey, *Phys. Rev.* **104,** 563 (1956).
23. E. O. Stejskal and J. E. Tanner, *J. Chem. Phys.* **42,** 288 (1965).
24. V. M. Kenkre, E. Fukushima, and D. Sheltraw, *J. Magn. Reson.* **128,** 62 (1997).
25. E. O. Stejskal, *J. Chem. Phys.* **43,** 3597 (1965).
26. J. E. Tanner and E. O. Stejskal, *J. Chem. Phys.* **49,** 1768 (1968).
27. B. Balinov, B. Jönsson, P. Linse, and O. Söderman, *J. Magn. Reson. A* **104,** 17 (1993).
28. A. Coy and P. T. Callaghan, *J. Chem. Phys.* **101,** 4599 (1994).
29. P. T. Callaghan, *J. Magn. Reson. A* **113,** 53 (1995).
30. J. E. M. Snaar and H. V. As, *J. Magn. Reson. A* **102,** 318 (1993).
31. O. Söderman and B. Jönsson, *J. Magn. Reson. A* **117,** 94 (1995).
32. A. Caprihan, L. Z. Wang, and E. Fukushima, *J. Magn. Reson. A* **118,** 94 (1996).
33. A. V. Barzykin, K. Hayamizu, W. S. Price, and M. Tachiya, *J. Magn. Reson. A* **114,** 39 (1995).
34. W. S. Price, A. V. Barzykin, K. Hayamizu, and M. Tachiya, *Biophys. J.* **74,** 2259 (1998).
35. M. H. Blees, *J. Magn. Reson. A* **109,** 203 (1994).
36. P. Linse and O. Söderman, *J. Magn. Reson. A* **116,** 77 (1995).
37. P. P. Mitra and B. I. Halperin, *J. Magn. Reson. A* **113,** 94 (1995).
38. L. Z. Wang, A. Caprihan, and E. Fukushima, *J. Magn. Reson. A* **117,** 209 (1995).
39. D. Sheltraw and V. M. Kenkre, *J. Magn. Reson. A* **122,** 126 (1996).
40. P. T. Callaghan, *J. Magn. Reson.* **129,** 74 (1997).
41. J. S. Murday and R. M. Cotts, *J. Chem. Phys.* **48,** 4938 (1968).
42. B. Robertson, *Phys. Rev.* **151,** 273 (1966).
43. C. H. Neuman, *J. Chem. Phys.* **60,** 4508 (1974).
44. J. Stepišnik, *Physica B* **104,** 350 (1981).
45. J. Stepišnik, *Physica B* **183,** 343 (1993).
46. C. H. Recchia, K. Gorny, and C. H. Pennington, *Phys. Rev. B* **54,** 4207 (1996).
47. P. W. Kuchel, A. J. Lennon, and C. Durrant, *J. Magn. Reson. B* **112,** 1 (1996).
48. A. V. Barzykin, *Phys. Rev. B* **58,** 14171 (1998).
49. P. M. Morse and H. Feshbach, "Methods of Theoretical Physics," McGraw–Hill, New York (1953).
50. K. Seki, A. V. Barzykin, and M. Tachiya, *J. Chem. Phys.* **110,** 7639 (1999).